Sixth International Symposium on Turbulence and Shear Flow Phenomena
Seoul, Korea, 22-24 June 2009

ROUGH CHANNELS

Paolo Orlandi
Dipartimento di Meccanica e Aeronautica
Via Eudossiana 16, Roma Italy
orlandi@kolmogorov.ing.uniroma1.it

ABSTRACT

Flows past rough surfaces are different from those past smooth walls and have been, in the past, studied experimentally because of their importance in several practical applications. Three regimes were observed, laminar, fully turbulent and transitional. The first one does not present any difference with that for smooth walls. In the second one has been observed experimentally that the resistance does not depend on the Reynolds number. A confirmation of this behaviour by DNS is not presently available, however the DNS has been used to understand the physics of rough flows. In particular it has been shown that the normal to the wall velocity fluctuations (u_2) play a fundamental role. In the present study the transitional regime, where the resistance depends on Re and on the shape of the obstacles, has been studied by DNS, and has been confirmed that also in this regime u_2 at the plane of the crests is the critical quantity.

INTRODUCTION

Nikuradse [1933] in his landmark paper on turbulent rough walls recalled the experimental results by Darcy [1858] and other scholars. The friction factor C_f appears in the Darcy formula which gives the resistance for any kind of conducts. To generate a chart with C_f in a function of ϵ/D (ϵ is a quantity representative of the roughness and D is the pipe radius) and the Reynolds number $Re = UD/\nu$, in the past, a large number of experiments were designed. Moody [1944] reported that Pigott [1933] analysed $10,000$ experiments in real pipes and that Nikuradse [1933] created artificial rough pipes. From these data von Karman [1931] derived theoretical formulae for the friction factor in the laminar ($C_f = C/Re$) and in the fully turbulent regime ($C_f = 1./(1.14 - 2log(\epsilon/D))^2$). However, von Karman [1946] in a different paper reported his clear vision of the near wall turbulence. At Pg.31, he wrote "the frictional resistance in smooth pipes can be regarded as a fictitious combination of resistances that correspond to the individual kinds of vortices. Assuming that a relationship exists between size of vortices and roughness." With today's knowledge this sentence means that to have a turbulent flow the near wall vortical structures must be generated and the roughness allows to vary their shape.

Nikuradse [1933] presented a large number of measurements in circular ducts with walls covered by sand grain; he showed that by plotting the friction factor versus the Reynolds number, three regimes are encountered: at low Re, the friction follows the law of laminar smooth walls, and does not depend on the roughness, at high Re, the friction depends on the kind of roughness, and not on Re. In the transitional regime, the friction depends on Re and on the kind of roughness. Moody [1944] wrote that the Nikuradse results in two regimes were satisfactory, and, instead, that these were not adequate for the transitional regime. This regime was analysed in detail by Colebrook & White [1937], concluding that the sharp transition observed by Nikuradse [1933] was difficult to reproduce. They suggested that the individual protuberances should play a role, and that a grain begins to contribute to the resistance when the local speed is large enough to shed eddies behind the obstacle. Colebrook & White [1937] from their results found a threshold value of the size of the grain in wall units equal to 14, which is comparable to the size of the streamwise vortices in the wall region of turbulent flows past smooth walls. At that time the physical interpretation was qualitative for the difficulty to perform detailed measurements. Bandyopadhyay [1987] was interested in the transitional regime of rough boundary layers, in particular for "k" type roughness observing that a fully turbulent regime is achieved when $k^+ > 40$ (k is the height of the square bars). The Direct Numerical Simulation can be a useful tool to understand the physics of transitional rough walls. The DNS, in fact, in the last years demonstrated its capability to produce a better comprehension of the fully turbulent regime, as it was shown by Leonardi *et al.* [2003a].

Regards the fully turbulent regime Nikuradse [1933] introduced the equivalent height K_S which is a quantity without an exact physical meaning, but useful and necessary for a good fit of the experimental data by the simple expression

$$U^+ = 8.48 + 5.75\log((y+\delta)/K_S), \qquad 5.75 = log_{10}/\kappa. \quad (1)$$

Several years later, for rough surfaces of simple shape, as square or two-dimensional rods, a classification of rough surfaces as "k" and "d" type was introduced by Perry *et al.* [1969]. In addition attempts were made to express the roughness function through a combination of geometrical parameters. We believe that it is important, as suggested by Belcher *et al.* [2003], to find a better parametrisation for rough surfaces, in particular dealing with real rough flows, as those in turbine blades, or in micrometereological applications. In predicting real flows, turbulence models are required, therefore, a better parametrisation could be achieved through the variables in the turbulence models, for instance the Reynolds stresses. These statistics, at the surface of the roughness, or better near the interface between the roughness and the flow depend on the shape of the surface. In a laboratory is rather difficult to measure the three velocity components, because the hot wire or the laser beam can not be located at the plane of the roughness crest. The measure of the other quantities, for instance the vorticity components and the pressure are even more difficult. The comprehension of all the details of the near wall physics relies on the DNS at low Reynolds number, but the DNS must be validated.

Orlandi *et al.* [2006] validated the numerical simulations by a comparison of the pressure distribution on two-dimensional rods, with that measured by Furuya *et al.*

[1976]. Experiments were also designed (Burattini *et al.* [2008]) to perform a detailed comparison of the statistics profiles and even of the spectra at low and high Reynolds number and the results were satisfactory. Regarding the flow physics, Leonardi *et al.* [2003a] explained why maximum drag is achieved for square bars at $w/k = 7$ (w is the separation between the square bars and k is the height of the elements). Moreover, Orlandi *et al.* [2003] demonstrated that, the normal velocity distribution on the plane of the crests is the driving mechanism for the modifications of the near wall structures. The preliminary results were suggesting that, a new parametrisation for rough flows could be obtained by $\tilde{u}'_2|_w$, with $\tilde{u}'_i = \langle u'^2_i \rangle^{1/2}$. (angular brackets $\langle\rangle$ indicate averages in the homogeneous directions and in time, and $|_w$ values at the plane of the crests). A continuous transition between smooth ($\tilde{u}'_2|_w = 0$) and rough walls ($\tilde{u}'_2|_w \neq 0$) is then reached, avoiding the sharp transition between "k" and "d" type rough surfaces. A useful parametrisation to be effective should lead to an expression for U^+, similar to Eq.(1), but K_S should be substituted by a quantity with a physical meaning, for example, a quantity controlling the near wall vortical structures. To have a wide validity the law should be verified for a large number of different rough surfaces; Orlandi & Leonardi [2006] for two- and three-dimensional roughness found a very good correlation between the roughness function ΔU^+ and $\tilde{u}'_2|_w$. This roughness function is different from that introduced by Hama [1954], as explained by Orlandi & Leonardi [2008], due to the different assumptions in the effective origin. A very simple formula relating $\tilde{U}^+$ to y^+ and $\tilde{u}'_2|_w$ was given in that paper.

It is important now to understand whether the $\tilde{u}'_2|_w$ can be an useful quantity to state when the transition between laminar and turbulent regimes occurs. This transition depends on the shape of the protuberances and the sand grain rough surfaces of Nikuradse [1933] are not appropriate, also for the lack of reproducibility. As done by Schlichting [1936)] three-dimensional elements of simple shape are considered. To understand even better the reasons of the transition isolated elements are inserted in one wall of the channel. The elements are not completely isolated because of the periodic conditions imposed, and it has been observed that the density distribution can play a role (Leonardi & Castro this proceedings). Isolated protuberances, however, show the formation of the near wall vortical structures and by varying the Reynolds number has been noticed that the Cooleridge & White [1937] observations were reproduced. An interesting relationship between the friction velocity and $\tilde{u}'_2|_w$ can be obtained. A solid obstacle is very common to promote the transition in boundary layers, and as it was postulated by von Karman [1946] this disturbance allows to understand the nature of turbulent friction.

Regards the transition from a laminar to a turbulent flow the DNS could give insights. For instance to create a turbulent flow in a channel or in a circular pipe usually a laminar Poiseuille velocity profile is assigned with random disturbances superimposed. This condition should generate the near wall structures. If the DNS uses a fine grid, the turbulent kinetic energy, initially distributed in all the scales, is dissipated, and the flow remains laminar also at high Reynolds numbers. By decreasing the resolution the dissipation decreases, and, then, the energy at the energy containing scales is sustained and the near wall structures form. At this point the resolution can be increased to perform a full DNS at the desired Reynolds number. To be clear in order to have a fully turbulent flow it is important to find a way to generate the streamwise vortices. This has been shown by Orlandi [2008] by temporal evolving simulations in channels and circular pipes, in an attempt to reproduce the Osborne Reynolds [1883] experiment. In the present study it has been shown that the DNS of channels with solid elements lead to fully turbulent flows without using the strategy before described.

Returning to the fully turbulent regime it is worth mentioning the different results obtained by the DNS which contributed to a better comprehension of the complex flow physics. The group in Roma produced a large number of papers by analysing the influence of rough surfaces and the differences between two- and three-dimensional surfaces. Bhaganar *et al.* [2004] considered an egg cartoon surface, that produces weak disturbances on the near wall structures, and as a consequence these remain coherent in the streamwise direction. Sen *et al.* [2007] by the Proper orthogonal decomposition method (POD) reached the same conclusions of Orlandi *et al.* [2006] that the roughness promote a turbulence isotropization in the near wall region. Coceal *et al.* [2006] considered staggered cubes, and by imposing free-slip conditions on the upper surface, they intended to reproduce flows close to those over urban roughness. Leonardi & Castro (in this proceedings) are analysing the effect of the density distribution of the cubic elements, explaining why there is a peak on the form drag.

Rough channels require a reduced amount of computational power with respect to boundary layers, this is the reason why only few simulations are available for boundary layers, and in particular those by Lee & Sung [2007]. Due to the high computational cost these authors considered two dimensional square bars with a ratio $w/k = 7$, the configuration which Leonardi *et al.* [2003a] found that was generating the largest form drag. Lee & Sung [2007] observed a reduction of the Reynolds stress anisotropy near the roughness as in rough channels (Leonardi *et al.* [2004]), and they concluded that the reduction depends on the type of roughness. The square bars with $w/k = 7$ can be considered by following the Perry *et al.* [1969] definition of "k" type, then it can be asserted that for "k" type roughness the isotropization is strong. For the "d" type geometries the structure anisotropy does not differ from that of smooth walls, and this was found by the Ashrafian & Anderson [2006] DNS. Leonardi *et al.* [2007] by analysing in detail the difference between "k" and "d" type roughness, concluded that the difference between "d"-type and "k"-type roughness is related to the relative magnitudes o the frictional and pressure drag. The classification of the roughness into two classes is inadequate, instead the parametrization before mentioned, linking the ΔU^+ to the $\tilde{u}'_2|_w$ allow to consider any kind of fully turbulent flow, including the smooth wall with $\tilde{u}'_2|_w = 0$.

From the results above mentioned it is clear that I believe that the DNS is a very efficient tool to study the flow physics near rough surfaces. This holds for smooth walls as it was demonstrated by del Alamo *et al.* [2004], but in these circumstances there is a strong Reynolds dependence, which requires a large amount of computational power. For rough walls the Reynolds independence shown by Nikuradse [1933]suggest that a lot can be learnt at low Reynolds number, but to understand the influence of the shape of the roughness a large number of simulations are necessary. From the numerical side a simple and accurate way to vary the shape of a body is based on the introduction of the immersed boundary technique in an efficient numerical method based on the use of an orthogonal grid. In the last years this approach become very popular and several different versions are available. Peskin [1972] introduced forces in the Navier-Stokes equations in order to have a zero velocity inside a solid body, but spurious oscillations were generated near the boundary. The main drawback was due to the necessity of small time steps, and, as a result three-dimensional simulations were not possible. The improvement described by Fadlun *et al.* [2000] received a lot of interest for the possibility to increase the Δt making possible the simulations of fully turbulent flows. To treat complex boundaries, in Fadlun *et al.* [2000], the velocities were set equal to zero in the solid, and, at the points closest to the boundary, were evaluated by linear interpolations. This assumption, for several flows is satisfactory because, near a solid boundary, the flow physics implies an almost linear velocity profile. An attempt was made to apply the linear interpolation to a turbulent channel with smooth walls, and a constant flow rate was not maintained. Leonardi & Orlandi [2004] modified the immersed boundary technique, for constant flow rate turbulent channels simulations with surfaces of any shape. An important constrain, however is the insertion of this technique in a robust Navier-Stokes solver, and the accurate staggered finite difference scheme (Orlandi [2000]) is very appropriate.

PHYSICAL AND NUMERICAL MODEL

The incompressible non-dimensional Navier-Stokes and continuity equations may be written as:

$$\frac{\partial U_i}{\partial t} + \frac{\partial U_i U_j}{\partial x_j} = -\frac{\partial P}{\partial x_i} + \Pi\delta_{i1} + \frac{1}{Re}\frac{\partial^2 U_i}{\partial x_j^2} \;; \quad \frac{\partial U_i}{\partial x_i} = 0 \;, \quad (2)$$

where Π is the pressure gradient required to maintain a constant flow rate, u_i is the component of the velocity vector in the i direction (1 indicates streamwise, 2 normal and 3 lateral directions) and p is the pressure. The reference velocity is the centerline laminar velocity profile U_P, the reference length is the half channel width h, hence in Eq.(2) t is a dimensionless time, and x_i are dimensionless coordinates. The Navier-Stokes equations have been discretized in an orthogonal coordinate system through a staggered central second-order finite-difference approximation. The discretization scheme of the equations is reported in chapter 9 of Orlandi [2000]. To treat complex boundaries, in fully turbulent channel flows Leonardi & Orlandi [2004] modified the immersed boundary technique by Fadlun *et al.* [2000]. In comparison with smooth channels, a large number of points is necessary to describe the contour of the rough surface. To maintain a constant flow rate Π, in Eq.(2), has to balance the friction and form drag. Π is evaluated during the calculation of the RHS_i (Right Hand Side) of Eq.(2). In a smooth channel, the staggered conservative scheme furnishes Π by the appropriate volume normalisation of the sum of RHS_1. In presence of rough walls, after the discrete integration of RHS_1 in the whole computational domain, to account for the metrics variations near the body a correction is necessary. This procedure requires a number of operations proportional to the number of boundary points, and the flow rate remains constant within round-off errors. In principle, there are not large differences in treating two- or three-dimensional geometries. However, in the latter case, a greater memory occupancy is necessary to define the nearest points to the surface.

A possible criticism of the capability of the method to deal with complex geometries is that, in contrast to methods based on a body fitted coordinate system (Orlandi 1989), an infinitely small resolution is needed. As the latter requirement is beyond our reach, the discrete representation of the roughness elements introduces small scale disturbances related to the grid size, since these disturbances are generated at a rather small local Reynolds number, they are rapidly dissipated and therefore are not important. These small disturbances in transitional flows are useful, because these are the disturbances producing the instability.

For fully turbulent flows the quality of the numerical method was demonstrated in Orlandi *et al.* [2006] by a comparison of the pressure distribution on the rods elements with that measured by Furuya *et al.* [1976]. They studied the boundary layer over two-dimensional circular rods, fixed to the wall transversely to the flow, for several values of w/k. The results presented for numerical validation, accounted for values of $w/k = 3, 7$ and 15; in addition, it is important to point out that circular rods are appropriate for numerical validation, due to the variation of the metric along the circle. The pressure accounts for the form drag which, for these values of w/k, overcomes the frictional drag. The numerical simulations for circular rods were performed, at $Re = U_P h/\nu = 4200$, in a channel with one wall smooth and the other rough. The rather good agreement implies that the numerical method is accurate and can be used to reproduce the flow past any kind of surface. From the physical point of view, the agreement between low Re simulations and high Re experiments (Furuya *et al.* [1976]) implies a similarity, in the near-wall region, between boundary layers and channel flows. In addition it can be asserted that, as in fully rough flows, (Nikuradse [1933]) a Reynolds number independence does exist. To our knowledge this detailed comparison between the pressure distribution on two-dimensional rods in rough boundary layers and in channel flows was never attempted.

RESULTS

Transition induced by a single roughness element

Difference between isolated and not-isolated.

Colebrook & White [1937] claimed that the individual elements of a rough boundary are important to understand the differences among smooth and rough walls. The anisotropy of smooth walls can be appreciated by the vertical profiles of the vorticity rms, which show the generation of the streamwise (ω_1) and normal (ω_2) components. From flow visualisations it has been observed an alternation of positive and negative longitudinal streaks of ω_2, which are longer than those of ω_1. Theoretical and numerical study described the formation of these structures starting from optimal disturbances, which, depending on the amplitude of the disturbance, can lead to linear or non-linear amplifications. In a laboratory a non-linear transition can be obtained by inserting a small solid element on a wall, which generates longitudinal vortices. These vortices depend on the inlet velocity profile and on the shape of the element. Several experiments can be found in the literature; one of the last by Velte *et al.* [(2008] considered a boundary layer as the incoming flow. In the present simulations a laminar Poiseuille velocity profile is imposed which produces a weak horseshoe vortex around the solid element on the lower wall. The strength of the horseshoe vortex increases by increasing the size of the obstacle and the Reynolds number. This has been demonstrated by the Kwang & Yanga [2004] DNS of flows in a channel with a cubic obstacle on a wall. In rough flows the flow structures generated by an obstacle interact with those

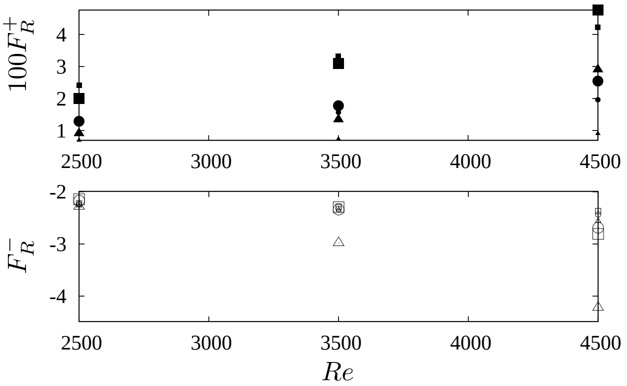

Figure 1: a)Positive contribution to the friction measured by the sum of $\omega_3|_w$ of opposite sign with respect to that of the incoming flow, b) negative contribution; large symbols for non-isolated, small for isolated elements, squares indicates cubic obstacles, circle cylinders, and triangle prisms.

produced by another obstacle. Numerically this interaction is reproduced by imposing the periodicity in the streamwise direction. The comparison of the periodic simulations with those obtained by inlet outlet boundary condition in a box of same length allows to understand the importance of the interaction. In fact at a certain Reynolds number these vortices attain sufficient extension to modify the basic flow impinging on the successive obstacle. We have considered three different planar geometries: square, circle and a triangle with the wedge pointing upstream all having height $k = 0.2$. Three bulk Reynolds numbers $Re_b = U_b 2H/\nu$ were assumed $2500, 3500$ and 4500, the simulations lasted for 24 time units. The lateral dimension of the channel are $4\pi \times \pi$ and the elements were described by a grid of 16×16 points.

The contour plots of ω_3 on the bottom wall show the effects of the obstacle on the friction drag distribution. $\omega_3|_w$ corresponds to the wall shear stress, usually visualised in a laboratory by oil streaks. The integral of this quantity on the wall surface shows whether the presence of the obstacle produces an increase of the friction drag. Indeed, it has been found that on the opposite smooth wall, for the three obstacles, there is no influence of the obstacle at any Reynolds number and the viscous drag is that due to the parabolic incoming profile ($F_S = 2$). The obstacle on the lower wall generates flow reversals with a change of sign for $\omega_3|_w$. Fig.1a shows that the favourable friction F_R^+ increases with Re and depends on the shape of the obstacle. F_R accounts only for the viscous drag. The small values of F_R^+ are due to the small areas of flow reversals. This figure in addition shows that there is a large difference between isolated (small symbols) and not-isolated (large symbols) elements, in the latter case the strength of the flow reversal is greater due to the disturbances of one element on the other. Even if the horseshoe vortex in front of the cube is bigger than that in front of the prism, the value of F_R^- for the cubic elements is smaller than that for the prism. This can be understood by the $\omega_3|_w$ contours in Fig.2a and Fig.2c. These figures show also that the recirculating regions behind the obstacle are bigger for the prisms than for the squares. The region of back flow behind the obstacle are generated by the strong vorticity layers near the vertical walls of the obstacle, which for the prism are stronger due to the flow acceleration from the stagnation point. From Fig.2a and Fig.2c. it is clear why, for not-isolated prisms, in Fig.1b F_R^- is bigger than for the not-isolated squares. Fig.2b and Fig.2d for isolated vortices explain why in this case there is a geometry independence of F_R^- at any Re.

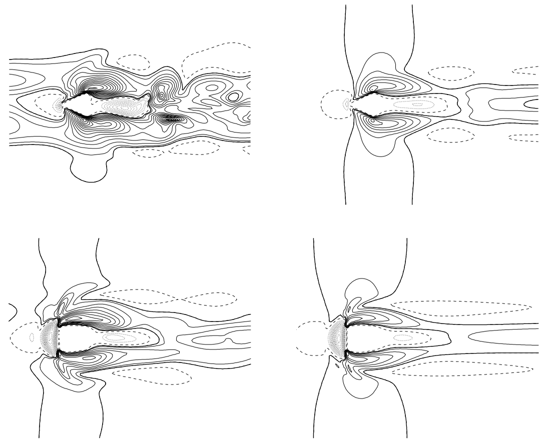

Figure 2: Distribution of $\omega_3|_w$ on the wall in a small region around the prism a) b) and the square c) d); a) c) isolated, b) d) not-isolated: solid negative $\Delta\omega_3|_w = -2$ for $-32 < \omega_3|_w < -4$, dashed negative $\Delta\omega_3|_w = -2$ for $-3 < \omega_3|_w < -1$, dotted positive $\Delta\omega_3|_w = 2$ for $2 < \omega_3|_w < 32$.

These results show that the critical Reynolds number depends on the incoming conditions, and that without disturbances the transition is delayed. The formation of streamwise vortices at a certain distance from the wall is a satisfactory way to detect whether the flow is laminar or turbulent. In the cases here analysed has been observed that at $Re = 3500$ for the triangular not-isolated elements in the region above the obstacle elongated structures of ω_2 form. These structure for the cube are weak and without the undulations necessary for the transition. From these simulations it can be concluded that for periodic distributions of solid elements the transition to turbulence is enhanced, and that the shape of the elements is important. In the next section the three regimes investigated by Nikuradse [1933] are discussed together with the influence of the shape of the elements.

Single elements

Elements of different shape with height and lateral side $k = h/H = 0.2$ have been inserted in a channel with the upper wall at $x_2 = 1$ and the lower wall at $x_2 = -(1 + k)$. At $t = 0$ the flow is above the elements, its Reynolds number defined as $Re = HU_P/\nu$ has been varied from $Re = 1500$ (laminar for all geometries) to $Re = 9600$ (fully turbulent). At this Re even if the resolution is marginal, a difference with the results at $Re = 4500$ can be appreciated. The elements considered are cylinders (C), cubes (S), forward prisms (P_f), backward prisms (P_b), transverse wedges (W_t), longitudinal wedges (W_l) half transverse wedges (H_t). In the transitional regime a first idea of the passage from laminar to turbulent flows is given by the time history of the friction velocity on the smooth wall (u_{τ_S}) and on the rough wall (u_{τ_R}). u_{τ_R} accounts for the viscous and form drag and can be evaluated by $u_{\tau_R}^2 \approx u_{\tau_S}^2 + (2 + k)|\Pi|$; Π is the mean pressure gradient maintaining the flow rate constant. This expression has been derived by assuming that the volume of the solid element is negligible with respect to the volume filled by the fluid. To understand whether the flow remains laminar or becomes turbulent it is convenient to plot the time histories of the friction coefficient $F_S = Reu_{\tau_S}$ and $F_R = Reu_{\tau_R}$. For laminar flows at any Re $F_S = 2$. At

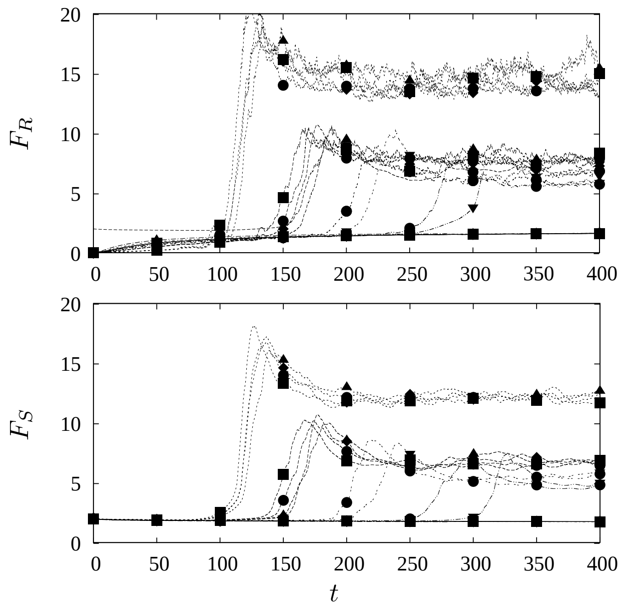

Figure 3: Time history of the friction factor on a) the smooth and b) on the rough wall: ● cylinder, ■cube, ▲back prism , ▼half transversal wedges, ——— $Re = 2500$, — - — $Re = 3000$, · $Re = 3500$, ···· $Re = 4500$, ········· $Re = 9600$.

$t = 0$ $F_R = 0$, it grows in time and for the laminar regime remains independent from Re and from the shape of the solid elements. These two quantities clearly show a large increase of the drag when the flow becomes turbulent.

Fig.3a shows that for any kind of geometry the flow remains laminar up to $Re = 2500$. A sharp increase of F_R indicates that transition occurs at different times and different Re, depending on the type of elements. The obstacle with a longitudinal wedge remain laminar for $Re = 4500$, implying that very small fluctuations of u_2 are produced by this element (the values are not reported in Fig.3). For H_t at $Re = 3000$ the flow becomes turbulent indicating that the flow acceleration in the ramp produces high fluctuations of u_2 which excite the formation of streamwise vortices in the layer above the element. These fluctuations perturb the opposite smooth wall, and Fig.3b shows that the flow becomes turbulent also at this low Re number, when it is rather difficult to generate a fully turbulent flow in a channel with two smooth walls. At $Re = 3500$, for H_t transition occurs at an early time. The simulations at $Re = 4500$ and $Re = 9600$ show that the square (S) is more unstable than the cylinder (C) and the forward prism (P_f).

According to Orlandi & Leonardi [2008] the driving mechanism of the roughness is $\tilde{u}_2'^+$. Then it is interesting to investigate whether also the transition can be related to $\tilde{u}_2'$. In the channels above described the lower wall can be considered a smooth wall with a localised periodic disturbance, which is different from the distributed disturbances considered by Orlandi & Leonardi [2008]. For the simulations in Fig.3, and for several others, at $t = 400$ $\tilde{u}_2'$ has been evaluated at the plane of the crests, and it has been normalised with respect to u_{τ_R}. Fig.4a shows that this quantity up to $Re = 2500$ remains small, and when the transition occurs, it jumps to higher values tending to 1 by increasing Re. In this figure are also reported the values of the maximum of $\tilde{u}_2'^+$ in a fully turbulent channel with two smooth walls at $R_\tau = 150, 180, 290$ and 580. From this figure it can be concluded that $\tilde{u}_2'^+$ can be considered the driving mechanism to produce the near wall vortical structures in wall turbulence. Colebrook & White [1937] claimed that the flow becomes turbulent when $k^+ > 14$. Fig.4b shows that our simulations confirm they observations; together with Fig.4a it can be asserted that to promote the transition it is necessary to insert an obstacle on a wall, the transition can be detected by a jump in $\tilde{u}_2'^+$. By increasing the Reynolds number if $k^+ > 14$ the flow becomes turbulent. The fully rough regime is established for $k^+ > 40$ with a rather good independence on the shape of the obstacle. The time signals on the two walls in Fig.3 indicate that near the rough walls higher frequencies are generated than those near the smooth wall, implying that the vortical structures near the rough wall are smaller.

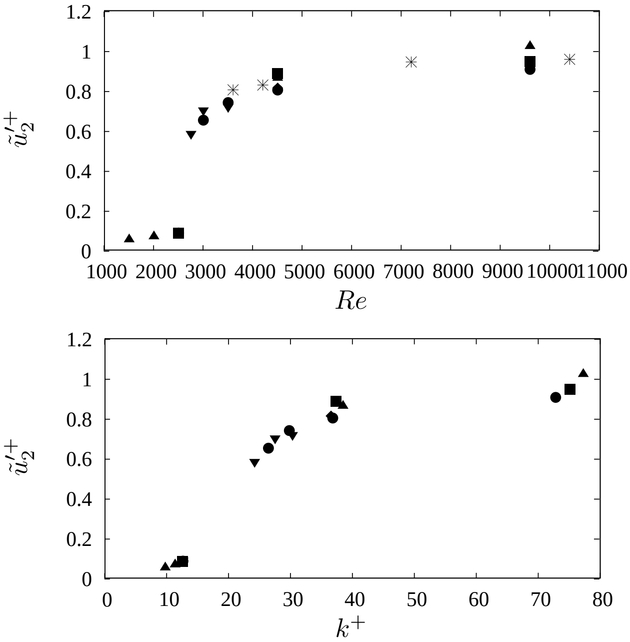

Figure 4: a) $\tilde{u}_2'^+$ versus Reynolds number, b) $\tilde{u}_2'^+$ versus k^+, symbols as in Fig.3, in a) the asterisk are given by the maximum of $\tilde{u}_2'$ for smooth walls.

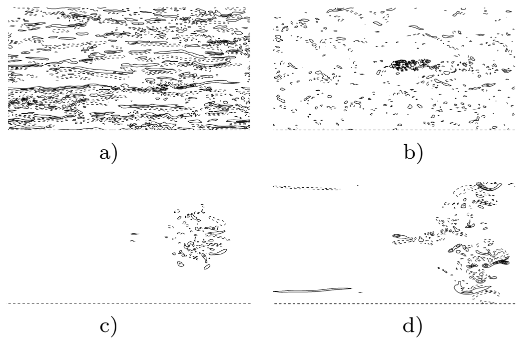

Figure 5: ω_2 contours in horizontal planes at $Re = 9600$ for the cylinder at: a) $x_2 = 0.95$ $t = 300$, b) $x_2 = -0.976$ $t = 300$, c) $x_2 = -0.976$ $t = 100$, d) square at $x_2 = -0.976$ $t = 100$; $\delta\omega_2 = 2$.

The formation of the near wall structures by the solid elements can be visualised by the contour plots of ω_2 in horizontal planes at $x_2 = -0.976$ a location close to the top of the elements. At $Re = 9600$ the grid may not resolve all the turbulent scales; however, Fig.5a shows that the energy containing scales, related to wall streaks near the smooth wall at $x_2 = 0.95$ are well resolved. It has been verified that the separation of the streaks is equal to 100 wall units. Fig.5b

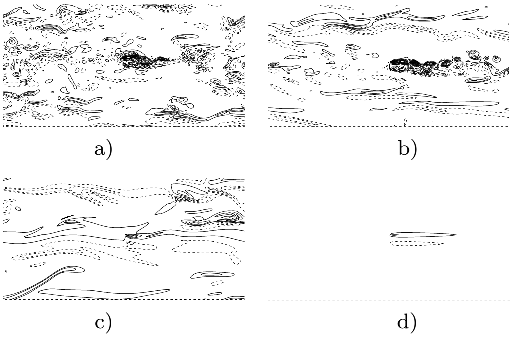

Figure 6: ω_2 contours in horizontal planes for the half transversal wedge at $x_2 = -0.976$ and $t = 300$ for: a) $Re = 4500$, b) $Re = 3500$, c) $Re = 3000$, d) $Re = 2500$, $\delta\omega_2 = 1$.

shows that, at $Re = 9600$, the cylindrical element generates shorter structures indicating a sort of turbulence isotropization near the rough surface. At this Re and at $t = 100$ it was found (Fig.3) that the sharp transition was not initiated, however, Fig.5c shows that the disturbance produced by the element are spreading, and that, at a certain distance, are clustered in a sort of turbulent spot. This complex structure travels and grows and in a short time fills the whole domain, at this point the transition ends and the fully turbulent regime is reached. From Fig.3 it can be speculated that at $t = 200$ the flow should not differ qualitatively from that at $t = 300$ and this has been observed by ω_2 contours not reported for lack of space. On the other hand, it has been found that at $t = 100$ the cubic element produces disturbances with a wider spreading (Fig.5d) in agreement with the early jump of F_R and F_S in Fig.3. The isotropization of the structures has been observed for the cubic element at $t = 200$ and $t = 300$. These flow visualisations indicate that there is an effect of the shape of the elements on the values of the transition Re number.

The effects of Re on the shape of the structures formation can be analysed by visualisations of the flow past the H_t obstacle at $Re = 4500, 3500, 3000$ and $Re = 2500$ at $t = 300$. Fig.3 shows that, at $Re = 2500$ the transition does not occur, at $Re = 4500$ transition occurs before $t = 300$, and that at $Re = 3000$ the jump in F_R starts at $t = 300$. The visualisations can explain this behaviour, in fact at $Re = 2500$, in the laminar regime, (Fig.6d) the element generates a small amount of ω_2 that decreases in the x_1 direction for the effect of the viscosity. The associated u'_2 fluctuations are weak and do not disturb the incoming flow. By reducing the viscosity ($Re = 3000$) the structures survive, spread and at $t = 300$ are weak and large (Fig.6c). At a later time these are thinner and similar to those produced at $Re = 3500$ (Fig.6b). The proof that the structures at $t = 400$ and $Re = 3000$ and those at $t = 300$ and $Re = 3500$ do not largely differ is given by the almost equal value of the resistance in Fig.3b. The small difference can be related to the greater intensity behind the elements and to the longer persistence. At $Re = 4500$ the tendency to form isotropic structures is depicted in Fig.6a.

Laminar and turbulent flows in wall bounded flows are characterised by a different friction factor $C_f = 2(u_\tau/U_b)^2$ as a function of the bulk Reynolds number $Re_b = U_b H/\nu$. For laminar flows $C_f = 12/Re_b$, instead for fully turbulent flows the more accepted law is $C_f = C Re_b^{-1/4}$, with $C \approx 0.07$; in the latter regime different laws were proposed (Patel & Head [1969]) which depend on the length of the channel before the measuring station. The transition between laminar and turbulent regimes as a function of Re_b is smooth. In the introduction it was mentioned that, for the simulations of transition in a channel with smooth walls, two different initial conditions can be derived by a flow field of fully turbulent flow at $R_\tau = 180$. One way consists on the imposition of the fully turbulent field at $t = 0$ and in finding the transition Re number by reducing the Re number. The transition Re is found when the turbulent kinetic energy decays and the laminar Poiseuille velocity profile is achieved. The simulations should evolve for very long time because this is a very slow process. The other way consists on the assumption of a laminar Poiseuille velocity profile and on the superimposition of the fluctuating field obtained by subtracting the mean velocity profile from the fully turbulent field at $R_\tau = 180$. With this initial condition the transitional Re number is found when the turbulent kinetic energy grows. The common character of these different initial conditions consists on the imposition of the structures of wall bounded flows. As it was before mentioned these structures are relevant, in fact by superimposing random disturbances both on a Poiseuille or on a mean turbulent velocity profile it is rather difficult to generate a fully turbulent flow. Fig.7 shows that the transition between laminar and turbulent flow is smooth, in the intermediate range of Re_b, minor differences in the values of C_f have been found, depending on the route chosen to detect the transition. However the two routes give the same values of Re_b when the laminar and the fully turbulent regimes are achieved. It is important to remind that in these simulations the disturbance is given at $t = 0$. In Fig.7 some of the laminar C_f (open circles) have been obtained by two-dimensional simulations with a Poiseuille profile and small random disturbances. The fully turbulent C_f (open squares) are obtained by the present finite difference scheme and by the pseudospectral method of Del Alamo *et al.* [2004] (open diamond). Both data agree with the theoretical laws.

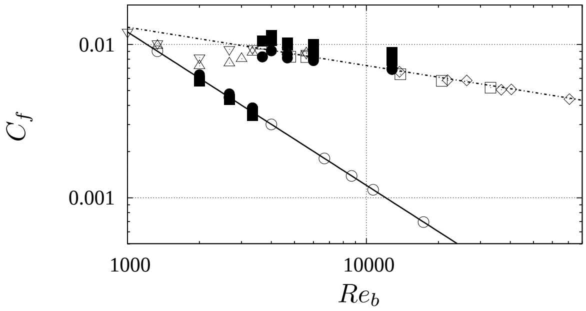

Figure 7: The resistance coefficient in function of the bulk Reynolds number for channels with smooth walls. □fully turbulent finite differences, ◇fully turbulent pseudospectral del Alamo *et al.* (2004), △transitional with fully turbulent at $t = 0$, ▽transitional with Poiseuille plus fluctuations, • smooth wall for channel with obstacle, ■wall with obstacle.

In the same figure the C_f of the channels with a solid element show that in the laminar regime the C_f follows the theoretical curve. To evaluate the C_f in these simulations it should be taken into consideration that the full channel height is $2+k$, and that at $t = 0$ the laminar flow is above the solid elements. The solid circles are evaluated at the upper and the solid squares at the lower wall with the obstacle. Fig.7 shows that for the channels with the solid obstacle there is a sharp transition between laminar and turbulent flows at Re_b between 3333 and 3666. This different trend

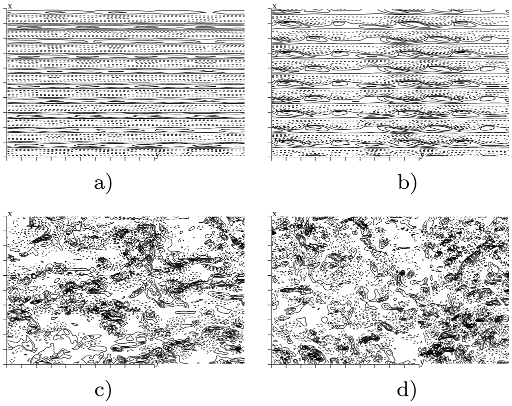

Figure 8: Contour plots of ω_2 at a distance k from the plane of the crests at $Re = 2000$ for: a) longitudinal wedges (W_l), b) cubes (S), c) transversal wedges (W_t), d) cubes (S); a) and b) at $t = 80$, c) and d) at $t = 240$, $\Delta\omega_2 = 0.5$.

of $C_f(Re_b)$ for the smooth and non-smooth channels is due to the production of fluctuations by the obstacle which are energising the outer flow. These fluctuations are due to the formation of vortical structures of size close to the dimensions of the obstacle. These vortical structures survive only at a certain Reynolds number, and, in particular, when their size is comparable to the thickness of the buffer layer as it is shown in Fig.4b. The simulations with one element explain clearly that the transition is caused by the generation and survival of the near wall structures. In presence of a single obstacle we have a geometrical set-up not too different from that of a channel with two smooth walls; this is the reason why the friction laws in Fig.7 do not differ from those for smooth walls. The friction laws change for rough disturbances uniformly distributed, as shown in the next section.

Big Distributed elements

To study the effects of a large number of elements a first set of simulations have been performed by putting elements with $k = 0.4$ and different forms in a channel of dimension $8H$ in the streamwise and $4H$ in the spanwise directions. Since the size of the elements is comparable to the size of the channel a low Re transition number as well as a strong dependence on the shape of the elements is expected. Staggered elements, in particular cylinders, cubes, transverse and longitudinal wedges have been considered. These are the same elements considered by Orlandi & Leonardi [2008] for fully rough turbulent flows. The size should have a large influence on the transitional process, then in the following section the analysis is repeated for $k = 0.2$.

Contour plots of ω_2 at a distance k from the plane of the crests show the effect of the shape of the roughness. In fact, for the longitudinal wedges (W_l) the disturbances emerging from the rough surface into the external field are weak and the flow, at $Re = 2000$, remains laminar (Fig.8a). To see better the vortex structures, in Fig.8, only part of the channel in the streamwise direction is visualised. For W_l the small disturbance are weak and these form elongated and ordered structures which do not promote the transition (Fig.8a). The amplitude of the disturbances produced by the square elements (S) increases and, at the same Reynolds number, undulations are generated (Fig.8b); these undulations are the precursors of the near wall structures in fully turbulent flows. The visualisation in Fig.8b is at $t = 80$ when the jump in the wall stress was starting (Fig.9a). In

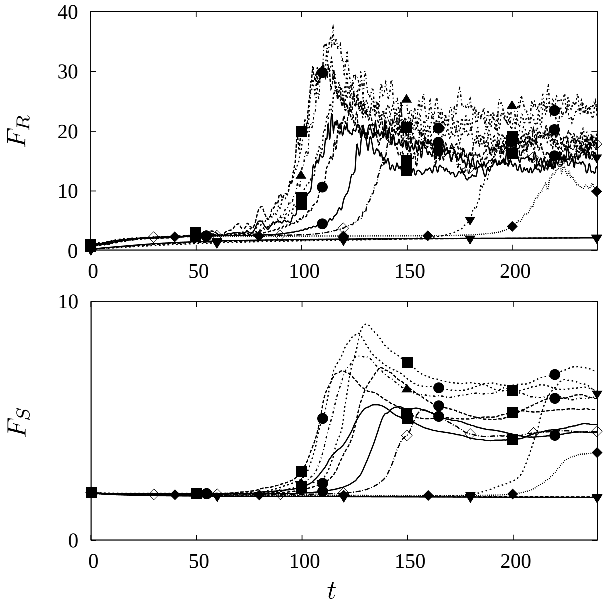

Figure 9: Time history of the resistance of: a) rough wall, b) smooth wall; • cylinder, ■cube, ▲transversal wedges, ▼longitudinal wedges, ——— $Re = 1600$, ···· $Re = 2000$, ········· $Re = 2800$, for W_t at $Re = 800$ ♦, ◇$Re = 1200$.

agreement with the flow visualisation, Fig.9a shows that for $Re = 2000$ the jump in the friction for W_l occurs at a greater time than for the squares (S). The transverse wedge elements (W_t) at $Re = 1200$ (ω_2 not shown) at $t = 120$ show three-dimensional ordered structures that approximately at $t = 140$ produce the jump in the total friction of the lower wall (Fig.9a). This geometry, among those here considered, gives the smaller transition Re number. When the flow is in a fully turbulent regime the structures at a distance k do not maintain the imprinting of the shape of the underlying elements and become isotropic as it emerges from the comparison between the contours in Fig.8c (W_t) and Fig.8d (S) obtained by the fields at $T = 240$.

As for the single elements the flow in a short interval of time goes from a laminar to a turbulent regime. The instability is generated near the rough surface, and, at any Re number, a strong interaction between the two walls occurs, and, therefore also the upper wall becomes turbulent. The transverse wedges produce a turbulent flow at $Re = 1200$ also near the smooth wall (Fig.9b). The achievement of a turbulent flow at this low Re is peculiar, but it could be expected because the channel can be considered a closed system with the disturbances propagating in any point of the field. At this low Re the structures near the smooth and the rough regions are rather different;this differences can be qualitatively appreciated by the different time fluctuations of the friction coefficients in Fig.9. The higher frequency in Fig.9a is characteristic of smaller vortical structures, which should be more isotropic. However, in Fig.10 the ω_2 visualisations give a more quantitative picture, where it appears that the high viscosity produces near the smooth wall fat ω_2 contours with a large degree of anisotropy (Fig.10b). The vortical structures are more isotropic near the rough wall (Fig.10a). The DNS demonstrate that the disturbances ejected from the rough surfaces reach the opposite smooth surfaces; here, these disturbances interacting with the appropriate mean shear, which depends on the Reynolds number, organise in structures that are fatter the smaller is Re

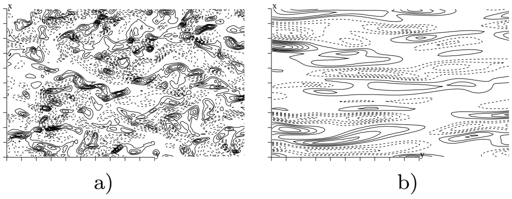

Figure 10: Contour plots of ω_2 for the transversal wedges (W_t) at: $Re = 1200$ for and $t = 240$: a) $x_2 = -0.947$, b) $x_2 = 0.954$; $\Delta\omega_2 = 0.5$.

(Fig.10b). This scenario has been often suggested for the transition, that is, that the disturbances in the outer region are those driving the transition from laminar to turbulent flows near a smooth wall. The near-wall structures, those producing the wall friction, are affected by the wall boundary conditions. Then, it can be asserted that, to control a turbulent flow the action should be made at the wall, for instance by changing the boundary condition of the velocity components. This has been demonstrated by Orlandi *et al.* [2003], where it was proved that among the three velocity components the normal velocity is the most important to mimic a rough surface.

The C_f versus Re_b for these surfaces composed by rather big elements indicates a different trend with respect to that found by Nikuradse [1933]; in fact, Fig.11a shows that the transition Re number depends on the shape of the elements. For instance also at the low $Re_b = 1066$ the transverse wedges (W_t) produce a turbulent flow on both walls. On the other hand the longitudinal wedges (W_l) up to $Re_b = 3000$ do not lead to a transition. The square (S) and the cylinders (C) produce friction factors slightly smaller than those by the transverse wedges (W_t). However by increasing the Reynolds number they tend to the same values. Fig.11a shows that at low Re_b the C_f of the smooth wall do not agree with the theoretical law, but that, instead, at high Re_b the agreement is good. The different trend at low and high Re_b is a consequence of the interaction between the two walls at low Re_b. To corroborate the observation that the u_2' at the plane of the crest affect the transition, in Fig.11b the profiles of $\langle \tilde{u_2'^2} \rangle^{1/2}$, scaled by the friction velocity of the rough wall, versus the distance from the plane of the crests $y = x_2 + 1$ shows that there is a threshold value. If $\tilde{u}_2'^+$ at $y = 0$ does not reach a value close to 1 the flow remain laminar. This quantity for rough flows has been suggested by Orlandi & Leonardi [2008] to be useful to find a new parametrization for the roughness function.

Small Distributed elements

The big elements discussed in the previous section were useful to investigate the shape and the Re dependence. Usually in the rough surfaces studied in laboratory experiments the size of the elements is rather small. Jimenez [2004] claimed that to understand the interaction between inner and outer layer $H/k > 50$; to perform DNS with this ratio a very large number of grid points are necessary. For $k = 0.4$ this ratio is 2.5, for $k = 0.2$ we are still far from 50 but at least a tendency can be analysed. For $k = 0.2$ a large number of simulations were performed in a substantial wide range of Reynolds numbers. The same shape of the elements considered in the previous section are used, but in this case further simulations with cubes followed by transversal wedges have been performed (this case is indicated by $2G$). The C_f in Fig.12 shows that, by reducing the size the cylinders, the flow remains laminar up to $Re_b = 8000$; instead, at this Re_b

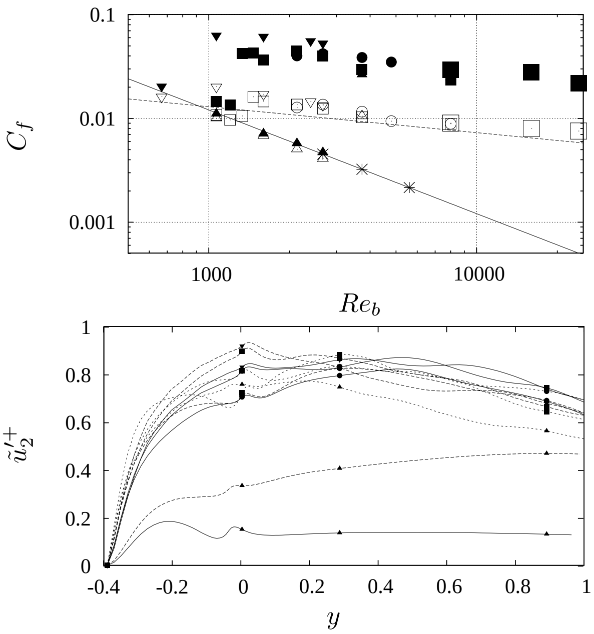

Figure 11: a) resistance coefficient versus the bulk Reynolds number for rough channels with elements of height $k = 0.4$, open symbols smooth wall, closed symbols rough wall: squares (S), circles (C), triangles (W_l), nablas (W_t), the asterisk smooth walls; b) $\tilde{u}_2'^+$ normal profiles: solid $Re = 1600$, dashed $Re = 2000$, chaindashed $Re = 2800$,

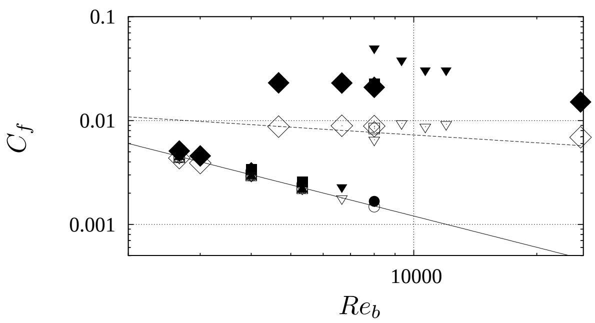

Figure 12: The resistance coefficient in function of the bulk Reynolds number for rough channels with elements of height $k = 0.2$, open symbols smooth wall, closed symbols rough wall: squares (S), circles (C), nablas (W_t), diamonds ($2G$),

for W_t the flow becomes turbulent. When two different kind of obstacles are inserted the transition to turbulence occurs at a smaller Re_b ($Re_b = 3500$). The set-up with two different kind of elements can be considered an attempt towards the simulations with random disturbances. The comparison between Fig.12 and Fig.11a demonstrates that with smaller elements the transition is delayed, and that in both cases it seems that the transition is sharp in agreement with the arguments by Colebrook & White [1937]. The comparison between the C_f versus Re_b for a single (Fig.7) and for distributed elements of same height (Fig.12) shows for the former a smaller transition Re_b. This can be explained because for the distributed elements there is of a reduction of the fluctuating velocities generated by the elements, and in particular of $\tilde{u}_2'^+$ at the plane of the crests.

FULLY TURBULENT FLOW

In this section is reported the analysis by Orlandi &

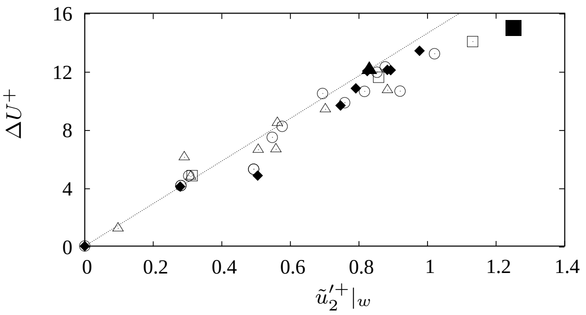

Figure 13: Roughness function versus the u_2' rms at the plane of the crests; □ Burattini *et al.* [2008], ◇ Orlandi & Leonardi [2008], ○ Leonardi *et al.* [2003a] △ Orlandi & Leonardi [2006], ▲Flores & Jimenez [2006], ■Cheng & Castro [2002].

Leonardi [2008] proposing a new parametrisation for fully turbulent rough flows. The new parametrisation intended to relate the roughness function to a flow variable to improve the Nikuradse [1933] parametrisation based on the equivalent sand grain roughness height K_S. This quantity does not have an exact physical meaning, but it is useful and necessary for a good fit of the experimental data. To find the new parametrisation have been in large part used numerical data, because of the easy evaluation of the necessary quantities at the roughness plane of the crests. Only two experiments were used, that by Cheng & Castro [2002] and that by Burattini *et al.* [2008]. The DNS allow to measure at the plane of the crest ($\tilde{y} = 0$) the mean streamwise velocity U_0 and $\tilde{u}_2'|_w$. The dimensionless friction velocity of the rough surface u_{τ_R} allows to evaluate $\tilde{U}^+ = (U - U_0)/u_{\tau_R}$ versus $\tilde{y}^+$. It was shown that for the different surfaces the following law holds

$$\tilde{U}^+ = \kappa^{-1} \ln(\tilde{y}^+) + B - \Delta U^+ \,, \tag{3}$$

with $k = 0.41$, $B = 5.5$, and ΔU^+ is the roughness function. Orlandi & Leonardi [2008], showed that, also at low Re, satisfactory long log-law regions are obtained, to evaluate ΔU^+.

Fig.13 shows that numerical and experimental data fit well with the relationship $\Delta U^+ = B/\kappa \tilde{u}_2'^+|_w$. For values of $\tilde{u}_2'^+|_w$ up to 0.8, the data agree well with the linear relationship, some disagreement is encountered at high $\tilde{u}_2'^+|_w$. In addition, Fig.13 establishes a limit on the value of the roughness function, which can be estimated as $\Delta U^+ \approx 15$. Without a correction at high $\tilde{u}_2'^+|_w$, Eq.(3) becomes

$$\tilde{U}^+ = \kappa^{-1} \ln(\tilde{y}^+) + B\left(1 - \frac{\tilde{u}_2'^+|_w}{\kappa}\right) \tag{4}$$

which can be useful in engineering applications.

Often the measure of the friction velocity is rather difficult, therefore Eq.(4) could be used to find the friction velocity u_{τ_R} measuring the mean velocity and the normal to the wall velocity rms at the crests plane. Equation (4) can be of greater help in simulations: in RANS (Reynolds Averaged Navier-Stokes) the Reynolds stresses equations are introduced, and often it is necessary to simulate the near wall region (low Reynolds number turbulence closures). The transport equation for the normal stress requires boundary conditions at the plane of the crests. By assigning $\tilde{u}_2'|_w$ Eq.(4) shows that we are mimicking a particular rough surface. The improvement with respect to the K_S approach consists on the fact that $\tilde{u}_2'|_w$ enters in the system of equations. On the same grounds, $\tilde{u}_2'|_w$ could be of help in engineering LES, to avoid the description of the real rough surfaces, which requires a large number of grid points, especially for three-dimensional surfaces. In these simulations, the resolved vertical fluctuations to assign at the plane of the crests should be evaluated through Eq.(4).

This new parametrisation suggests that profiles of statistics related to $\tilde{u}_2'$ account for the complex physics of the thin layer near the plane of the crests. This corroborate the results obtained for the transitional regime where it was demonstrated that a fully rough regime is obtained when the peak value of $\tilde{u}_2'^+$ is close to 1.

CONCLUSIONS

This paper is devoted to increase our knowledge of rough turbulent flows in channels. The channels allow to reduce the amount of computational power and the physics does not differ from that in circular pipes or boundary layers. The previous numerical simulations were focused on the fully turbulent regime at intermediate Reynolds numbers. The same numerics can be applied to increase the Reynolds number to see whether the friction factor Re independence observed experimentally by Nikuradse [1933] is reproduced. To this purpose an enormous amount of computational time is necessary also because of the necessity to perform the simulations with different rough surfaces. Personal clusters on the other hand allows to perform simulations devoted to understand the transitional regime where the friction factor is Re and roughness dependent. Also in this regime to perform the same number of numerical experiments as those reported by Nikuradse [1933] is a rather hard task. The study has been limited to simulations with a single and with distributed solid elements. In the former conditions the element is necessary to generate the velocity fluctuations leading to a turbulent flow and the friction coefficient agrees with the theoretical and empirical laws. For flows past distributed elements has been observed that the transition from laminar to turbulent flows is sharp, that is, it occurs at a well defined Reynolds number, which strongly depends on the size and shape of the solid elements. In agreement with the results for the fully turbulent regime it has been found that the most relevant physical quantity to promote the transition is the normal velocity rms at the plane of crests. Only if $\tilde{u}_2'^+$ is close to 1 it is possible to have a fully turbulent rough flow. Flow visualisations of ω_2 have shown that near the roughness for laminar flows the vortical structures are ordered and that for turbulent flows these becomes more isotropic and then are completely different from the near wall structures near smooth walls. The simulations of rough surfaces with a random shape is rather difficult, but by considering a surface with two different kind of elements has been observed that the transitional Re number is drastically reduced.

ACKNOWLEDGEMENTS

The support of a MIUR 60 % grant is acknowledged. Computational time was given by CASPUR. Several simulations were performed in the Portorico cluster and in the DMA clusters bought by PRIN resources. Discussions with Leonardi, Antonia, and Burattini are greatly appreciated.

REFERENCES

Ashrafian, A. & Andersson, H. I., 2006a , "The structure of turbulence in a rod-roughened channel" *Intl J. Heat Fluid Flow* Vol. 27, 65-79.

del Alamo, J.C., Jimenez, J., Zandonade, P. & Moser, R.D., 2004, "Scaling of the energy spectra of turbulent channels"

J. Fluid Mech. Vol. 500, 135–144.

Bandyopadhyay, P.R., 1987, "Rough–wall turbulent boundary layers in the transition regime" *J. Fluid Mech.* 180, 231–266.

Belcher, S.E., Jerram, N. & Hunt, J.C.R., 2003, "Adjustment of a turbulent boundary layer to a canopy of roughness elements" *J. Fluid Mech.* Vol. 488, 369–398.

Bhaganagar, K., Kim, J. & Coleman, G., 2004, "Effect of roughness on wall-bounded turbulence" *Flow Turbulence and Combustion.* Vol. 72 , 463–492.

Burattini, P., Leonardi, S., Orlandi, & Antonia, R.A., 2008, "Comparison between experiments and direct numerical simulations in a channel flow with roughness on one wall" *J.Fluid Mech.* Vol. 600 pp.403 –426 .

Cheng, H., & Castro, I.P., 2002, "Near wall flow over urban-like roughness." *Boundary-Layer Met.*, Vol. 104, pp. 229-259.

Coceal, O., Thomas, T.G., Castro, I.P. & Belcher, S.E., 2006, "Mean flow and turbulence statistics over groups of urban- like cubical obstacles." *Boundary-Layer Met.*, Vol. 121, 491-519.

Colebrook, C.F. & White, C.M., 1937, "Experiments with fluid friction in roughned pipes" *Proc. Roy. Soc. A* Vol. 161, pp. 367–381.

Darcy, H., 1858, "Recherches experimentales relatives au movement de l'eau dans les tuyaux" *Memoires a l'Academie d. Sciences de l'Institute de France*

Fadlun, E. A., Verzicco, R., Orlandi, P. & Mohd-Yusof, J., 2000, "Combined immersed boundary finite-difference methods for three-dimensional complex flow simulations." *J. Comput. Phys.* Vol. 161, 35–60.

Flores, O. & Jimenez, J., 2006, "Effect of wall-boundary disturbances on turbulent channel flows" *J. Fluid Mech.* Vol. 566, 357–376.

Furuya, Y., Miyata, M. & Fujita, H., 1976, "Turbulent boundary layer and flow resistance on plates roughened by wires." *J. Fluids Eng.* Vol. 98, 635–644.

Hama, F. R., 1954, "Boundary layer characteristics for smooth and rough surfaces." *Trans. Soc. Naval Archit. Mar. Eng.* Vol. 62, 333–358.

Jiménez, J., 2004, "Turbulent flows over rough walls" *Ann. Review of Fluid Mech.* Vol. 36, 173–196.

Karman von, Th., 1931, "Mechanical similitude and Turbulence" *NACA Tech. Memorandum 601*

Karman von, Th., 1946, "On laminar and turbulent friction" *NACA Tech. Memorandum 1092*

Kwang, J.Y. & Yanga K.S., 2004, "Numerical study of vortical structures around a wall-mounted cubic obstacle in channel flow" *Phys. Fluids* Vol. 16 pp.2382–2394.

Lee, S.H. & Sung, H.J., 2007, "Direct numerical simulation of the turbulent boundary layer over a rod-roughened wall" *J.Fluid Mech.*, Vol. 584 pp.125–146.

Leonardi S. & Orlandi P., 2004, "A numerical method for turbulent flows over complex geometries" *ERCOFTAC bullettin* Vol. 62, 41-46.

Leonardi, S., Orlandi, P., Smalley R.J., Djenidi, L. & Antonia, R. A., 2003, "Direct numerical simulations of turbulent channel flow with transverse square bars on the wall" *J. Fluid Mech.* Vol. 491 , 229 - 238.

Leonardi, S., Orlandi, P., Djenidi, L. & Antonia, R.A., 2004, "Structure of turbulent channel flow with square bars on one wall" *Int. J. Heat and Fluid Flow*, Vol. 25, 384–392.

Leonardi, S., Orlandi, & Antonia, R.A., 2007, "Properties of d and ktype roughness in a turbulent channel flow" *Physics of Fluids.* Vol. 19, pp. 12501–6.

Moody, L.F., 1944, "Friction factors for pipe flow" *Trans. ASME* Vol.66 pp.671–678.

Nikuradse, J. , 1933, "Laws of flow in rough pipes" NACA TM 1292 (1950).

Orlandi, P., 1989, "Numerical solution of 3-D flows periodic in one direction and with complex geometries in 2-D" *Annual Research Briefs, Center for Turbulence Research 1989*, 215-230.

Orlandi, P., 2000, *Fluid Flow Phenomena : A Numerical Toolkit*, Dordrecht, Kluwer.

Orlandi, P., 2008, "Time evolving simulations as a tentative reproduction of the Reynolds experiments on flow transition in circular pipes" *Physics of Fluids.* Vol. 20, pp.101516–12.

Orlandi P., & Leonardi S., 2006, "DNS of turbulent channel flows with two– and three–dimensional roughness" *Journal of Turbulence* Vol. 7, No. 53.

Orlandi P., & Leonardi S., 2008, "Direct numerical simulation of three-dimensional turbulent rough channels: parameterization and flow physics" *J. Fluid Mech.* Vol. 606, pp. 399-415.

Orlandi P., Leonardi S., Tuzi R. & Antonia R.A., 2003, "DNS of turbulent channel flow with wall velocity disturbances" *Phys. Fluids.* Vol. 15, 3497–3600.

Orlandi P., Leonardi S., & Antonia R.A., 2006, "Turbulent channel flow with either transverse or longitudinal roughness elements on one wall" *J. Fluid Mech.* Vol. 561, pp. 279-305.

Patel, V.C. & Head, M.R., 1969, "Some observations on skin friction and velocity profiles in fully developed pipe and channel flows" *J. Fluid Mech.* Vol. 38, pp. 181–201.

Perry, A. E., Schofield, W. H. & Joubert, P. N., 1969, "Rough wall turbulent boundary layers" *J. Fluid Mech.* Vol. 37, 383–413.

Peskin, C.S., 1972, "Flow patterns around heart valves: a numerical method" *J. of Comp. Phys.*,Vol. 10, 252–271.

Pigot, R.J.S., 1933, "The flow of fluids in closed conduits" *Mechanical Engineering* Vol. 55, pp. 497–501.

Reynolds O. 1883. "An experimental investigation of the circumstances which determine whether the motion of water in parallel channels shall be direct or sinuous and of the law of resistance in parallel channels" *Philos. Trans. R. Soc.*, Vol. 174, pp. 93582

Schlichting, H., 1936, "Experimental investigation of surface roughness" NACA-TM.823

Sen,M., Bhaganagar, K. & Juttijudata, V., 2007, "Application of Proper Orthogonal Decomposition (POD) to investigate turbulent boundary layer in a channel with rough-walls" *Journal of Turbulence* Vol. 8, No.41.

Velte, C.M., Hansen, M.O.L. & Okulov, V.L., 2008, "Helical structure of longitudinal vortices embedded in turbulent wall-bounded flow" *J. Fluid Mech.* Vol. 619, pp. 167–177.